Cellular/Molecular

Densin-180 Controls the Trafficking and Signaling of L-Type Voltage-Gated $Ca_v1.2$ Ca^{2+} Channels at Excitatory Synapses

Shiyi Wang,[1] Ruslan I. Stanika,[2] Xiaohan Wang,[3] Jussara Hagen,[1] Mary B. Kennedy,[4] Gerald J. Obermair,[2] Roger J. Colbran,[3] and Amy Lee[1,5,6]

[1]Department of Molecular Physiology and Biophysics, University of Iowa, Iowa City, Iowa 52242, [2]Division of Physiology, Medical University Innsbruck, 6020 Innsbruck, Austria, [3]Department of Molecular Physiology and Biophysics and the Brain Institute, Vanderbilt University, Nashville, Tennessee 37235, [4]Department of Biology, California Institute of Technology, Pasadena, California 91125, [5]Department of Otolaryngology Head-Neck Surgery, University of Iowa, Iowa City, Iowa 52242, and [6]Department of Neurology, University of Iowa, Iowa City, Iowa 52242

Voltage-gated $Ca_v1.2$ and $Ca_v1.3$ (L-type) Ca^{2+} channels regulate neuronal excitability, synaptic plasticity, and learning and memory. Densin-180 (densin) is an excitatory synaptic protein that promotes Ca^{2+}-dependent facilitation of voltage-gated $Ca_v1.3$ Ca^{2+} channels in transfected cells. Mice lacking densin (densin KO) exhibit defects in synaptic plasticity, spatial memory, and increased anxiety-related behaviors—phenotypes that more closely match those in mice lacking $Ca_v1.2$ than $Ca_v1.3$. Therefore, we investigated the functional impact of densin on $Ca_v1.2$. We report that densin is an essential regulator of $Ca_v1.2$ in neurons, but has distinct modulatory effects compared with its regulation of $Ca_v1.3$. Densin binds to the N-terminal domain of $Ca_v1.2$, but not that of $Ca_v1.3$, and increases $Ca_v1.2$ currents in transfected cells and in neurons. In transfected cells, densin accelerates the forward trafficking of $Ca_v1.2$ channels without affecting their endocytosis. Consistent with a role for densin in increasing the number of postsynaptic $Ca_v1.2$ channels, overexpression of densin increases the clustering of $Ca_v1.2$ in dendrites of hippocampal neurons in culture. Compared with wild-type mice, the cell surface levels of $Ca_v1.2$ in the brain, as well as $Ca_v1.2$ current density and signaling to the nucleus, are reduced in neurons from densin KO mice. We conclude that densin is an essential regulator of neuronal Ca_v1 channels and ensures efficient $Ca_v1.2$ Ca^{2+} signaling at excitatory synapses.

Key words: excitatory; postsynaptic; trafficking

Significance Statement

The number and localization of voltage-gated Ca_v Ca^{2+} channels are crucial determinants of neuronal excitability and synaptic transmission. We report that the protein densin-180 is highly enriched at excitatory synapses in the brain and enhances the cell surface trafficking and postsynaptic localization of $Ca_v1.2$ L-type Ca^{2+} channels in neurons. This interaction promotes coupling of $Ca_v1.2$ channels to activity-dependent gene transcription. Our results reveal a mechanism that may contribute to the roles of $Ca_v1.2$ in regulating cognition and mood.

Introduction

Ca^{2+} influx through voltage-gated (Ca_v) $Ca_v1.2$ L-type Ca^{2+} channels regulates neuronal excitability (Lacinova et al., 2008), synaptic plasticity (Moosmang et al., 2005), and learning and memory (Moosmang et al., 2005; White et al., 2008). Like other Ca_v channels, $Ca_v1.2$ is composed of a pore-forming α_1 subunit ($Ca_v1.2$) and auxiliary β and $\alpha_2\delta$ subunits (Simms and Zamponi, 2014). The *CACNA1C* gene encoding $Ca_v1.2$ is a major risk gene for multiple neuropsychiatric disorders, including autism spectrum disorder, attention deficit–hyperactivity disorder, schizophrenia, bipolar disorder, and major depression (Cross-Disorder Group of the Psychiatric Genomics Consortium, 2013). Therefore, an understanding of the factors regulating $Ca_v1.2$ is crucial for understanding the balance between normal and disordered states of cognitive and affective processing.

Received Aug. 11, 2016; revised March 23, 2017; accepted March 27, 2017.

Author contributions: S.W., R.I.S., X.W., G.J.O., and A.L. designed research; S.W., R.I.S., and X.W. performed research; J.H., M.B.K., and R.J.C. contributed unpublished reagents/analytic tools; S.W., R.I.S., X.W., and G.J.O. analyzed data; S.W. and A.L. wrote the paper.

This work was supported by the National Institutes of Health (Grants DC009433 and NS084190 to A.L.; Grants NS17660 and NS 028710 to M.B.K.; and Grant MH063232 to R.J.C.), a Carver Research Program of Excellence Award to A.L.; the American Heart Association (Grant 14PRE18420020 to X.W.); the Austrian Science Fund (Grants P24079 and F4415 to G.J.O.); the G. and B. Moore Foundation (M.B.K.), and the Howard Hughes Medical Institute (M.B.K.). We thank J. Hell for providing cDNAs and M. Joiner and other members of the Lee and Colbran laboratories for valuable input. The content is solely the responsibility of the authors and does not necessarily represent the official views of the NIH or other funding agencies.

The authors declare no competing financial interests.

Correspondence should be addressed to Amy Lee, Department of Molecular Physiology and Biophysics, University of Iowa, PBDB 5318, 169 Newton Road, Iowa City, IA 52242. E-mail: amy-lee@uiowa.edu.

DOI:10.1523/JNEUROSCI.2583-16.2017

 0270-6474/17/374679-13$15.00/0

In addition to interactions with auxiliary subunits, neuronal $Ca_v1.2$ channels interact with a variety of other regulatory proteins (Calin-Jageman and Lee, 2008; Lipscombe et al., 2013). The distal C terminus of $Ca_v1.2$ contains a consensus site for binding to proteins containing Postsynaptic Density-95, *Drosophila* Discs-Large and Zona Occludens (PDZ) domains (Kurschner and Yuzaki, 1999; Weick et al., 2003). The related $Ca_v1.3$ channel also contains a C-terminal PDZ-binding site, which serves as a ligand for multiple proteins that regulate the function of these channels (Olson et al., 2005; Zhang et al., 2005; Calin-Jageman et al., 2007; Jenkins et al., 2010; Gregory et al., 2011; Gregory et al., 2013). Although several PDZ domain-containing proteins are known to interact with $Ca_v1.2$ (Kurschner et al., 1998; Kurschner and Yuzaki, 1999), the functional consequences of such interactions have not been characterized.

Densin-180 (densin) is a leucine-rich repeat and PDZ domain-containing protein that is enriched in the postsynaptic density of excitatory synapses and interacts with a variety of postsynaptic proteins including calmodulin-dependent protein kinase II (CaMKII; Apperson et al., 1996; Strack et al., 2000; Walikonis et al., 2001). We showed previously that the PDZ domain of densin interacts with $Ca_v1.3$ and recruits CaMKII to the channel complex, which causes Ca^{2+}-dependent facilitation of $Ca_v1.3$ currents in transfected cells (Jenkins et al., 2010). However, mice lacking densin (densin KO) display defects in spatial memory and elevated anxiety levels (Carlisle et al., 2011), which are more similar to the behavioral phenotypes in mice lacking $Ca_v1.2$ (Moosmang et al., 2005; Lee et al., 2012) than in mice lacking $Ca_v1.3$ (Pinggera and Striessnig, 2016). Together with evidence that $Ca_v1.2$ is more abundant in the brain than $Ca_v1.3$ (Clark et al., 2003), these results suggest that densin may be a physiological relevant component of $Ca_v1.2$ complexes.

To test this hypothesis, we investigated whether densin functionally interacts with $Ca_v1.2$ in transfected cells and in neurons. We found that densin binds to, but differentially modulates, $Ca_v1.2$ compared with $Ca_v1.3$. Densin enhances the cell surface density and postsynaptic clustering of $Ca_v1.2$, as well as coupling of $Ca_v1.2$ to phosphorylation of the transcription factor cAMP response element binding protein (CREB). Our results underscore the importance of $Ca_v1.2$–protein interactions for neuronal Ca^{2+} signaling, which should be considered in the context of how alterations in $Ca_v1.2$ channel function may lead to neuropsychiatric disease.

Materials and Methods

Animals. All procedures using animals were performed in accordance with the University of Iowa Institutional Animal Care and Use Committee. The densin KO mouse line was bred on a C57BL/6 background and has been described previously (Carlisle et al., 2011). Mice were housed three or four per cage and maintained on a 12 h reverse light/dark cycle with *ad libitum* access to food and water.

cDNAs. For cell transfection, cDNAs corresponding to $Ca_v1.2$ subunits [rbcII (GenBank #M67515), β_{2a} (GenBank #NC013684) and $\alpha_2\delta_1$ (GenBank #M76559.1)] were expressed from the pcDNA3.1+ vector (Invitrogen). The following constructs were described previously: $Ca_v1.2$/pcDNA3.1+ (FLAG-tagged), $Ca_v1.2\Delta$NT/pcDNA3.1+ (FLAG-tagged) lacking aa 1–109, GST-tagged $Ca_v1.2$ intracellular domains: NT (aa 1–124); loop I-II (aa 406–524); loop II-III (aa 754–902); loop III-IV (aa1170–1222); CT (aa 1942–2144) (Zhou et al., 2004; Zhou et al., 2005); GST-tagged C-terminal domain of $Ca_v1.3$ (aa 1962–2155) (Calin-Jageman et al., 2007); GFP-tagged densin (GenBank #NM_057142.1 (Jiao et al., 2008)); pβA-eGFP and pβA-$Ca_v1.2$-hemagglutinin (HA) (Altier et al., 2002; Obermair et al., 2004). GST-tagged fragments of $Ca_v1.2$ NT were generated by PCR amplification and subcloning into BamHI and EcoRI sites of pGEX-4T1. The pβA-$Ca_v1.2$-HA-ΔNT was generated by PCR amplification of the sequence encoding $Ca_v1.2$-HA-ΔNT using pβA-$Ca_v1.2$-HA as a template and subcloning the sequence encoding $Ca_v1.2\Delta$NT into HindIII and XbaI sites of the pβA empty vector. To generate $Ca_v1.2\Delta$B1a/pcDNA3.1+, the sequence corresponding to the B1a region (aa 65–76) was deleted from $Ca_v1.2$/pcDNA3.1+ using site-directed mutagenesis. The SNAP-tagged-$Ca_v1.2$ construct was generated by amplifying the $Ca_v1.2$-HA coding region in pβA-$Ca_v1.2$-HA and ligating into *PmeI* and NotI sites of the pSNAPr vector (New England Biolabs) using the NEBuilder HiFi DNA Assembly cloning system (New England BioLabs).

Cell culture and transfection. Human embryonic kidney cells transformed with SV40 T-antigen (HEK293T; American Type Culture Collection catalog #CRL-3216, RRID: CVCL_0063) were maintained in DMEM (Thermo Fisher Scientific) with 10% fetal bovine serum at 37°C in a humidified atmosphere with 5% CO_2. Cells were grown to 70–80% confluence and transfected with Gene Porter reagent (Genlantis) or Fugene 6 (Promega) according to the manufacturer's protocols. For electrophysiology, cells were plated in 35 mm dishes and transfected with $Ca_v1.2$ subunit cDNAs: $Ca_v1.2$ (1.5 μg), β_{2a} (1 μg), and $\alpha_2\delta_1$ (1 μg). pEGFPN1 (0.1 μg) or GFP-densin (1 μg) was cotransfected, which facilitated identification of transfected cells by fluorescence. For pull-down assays, cells were plated in 60 mm dishes and transfected with GFP-densin (6 μg). For coimmunoprecipitation experiments, cells were plated in 60 mm dishes and transfected with $Ca_v1.2$ (2.4 μg), β_{2a} (0.8 μg), $\alpha_2\delta_1$ (0.8 μg), pEGFPN1 (0.5 μg), and pcDNA (3.5 μg) or GFP-densin (4 μg).

In vitro *binding assays.* GST-fusion proteins containing intracellular domains of $Ca_v1.2$ were expressed in *E. coli* (BL21) and purified on glutathione-Sepharose (GE Healthcare Life Sciences) according to standard protocols. HEK293T cells transfected with GFP-densin (4 μg) were harvested and homogenized in ice-cold cell lysis buffer containing 50 mM Tris-HCl, 150 mM NaCl, 1% Triton X-100, 0.25% w/v sodium deoxycholate, 1 mM EDTA, pH 7.4, and protease inhibitors. The homogenate was rotated at 4°C for 1 h to solubilize membrane proteins and the insoluble material was separated by centrifugation at 16,100 × *g* for 30 min. The supernatant was incubated with immobilized GST fusion proteins (50% slurry) at 4°C overnight. The beads were washed three times with ice-cold cell lysis buffer and the bound proteins were eluted with SDS-containing sample buffer, subjected to SDS-PAGE, and transferred to nitrocellulose. Western blotting was with mouse monoclonal anti-GFP (1:3000, Santa Cruz Biotechnology catalog #sc-53882, RRID: AB_783653).

Coimmunoprecipitation assays. Transfected HEK293T cells were harvested 48 h after transfection. Cell lysates were prepared as described for binding assays and incubated with FLAG-agarose beads (50% slurry; Sigma-Aldrich) overnight, rotating at 4°C. After three washes with cell lysis buffer, proteins were eluted and analyzed by SDS-PAGE. Coimmunoprecipitated proteins were detected by Western blotting with GFP antibodies (1:3000, Santa Cruz Biotechnology catalog #sc-53882, RRID: AB_783653). For coimmunoprecipitation from mouse brain, neural tissue was subjected to subfractionation according to previously described methods (Cox and Emili, 2006). The prefrontal cortex was dissected and homogenized in lysis buffer containing the following (in mM): 250 sucrose, 50 Tris-HCl, 5 $MgCl_2$, and 1 DTT, pH 7.4, plus protease inhibitors. The nuclear fraction was removed by centrifugation at 800 × *g* for 15 min and the supernatant was subjected to ultracentrifugation at 100,000 × *g* for 1 h. The membrane pellet was solubilized in solubilization buffer containing 50 mM Tris-HCl, 150 mM NaCl, pH 7.5, 1% Triton X-100, and protease inhibitors) at 4°C for 30 min and the insoluble material was removed by ultracentrifugation at 100,000 × *g* for 1 h. Either rabbit control IgG (Sigma-Aldrich catalog #I5006, RRID: AB_1163659) or anti-$Ca_v1.2$ antibodies (5 μg) were added to the solubilized membrane proteins along with Protein A Sepharose (50% slurry, Sigma-Aldrich). Reactions were continued overnight with end-over-end rotation at 4°C. The resin was collected by centrifugation and rinsed three times with solubilization buffer. Bound proteins were eluted, resolved on a SDS-polyacrylamide gel (4–12%), and Western blotted with anti-densin antibodies (1:5000, Colbran laboratory at Vanderbilt University, catalog #Ab650, RRID: AB_2619660; Jiao et al., 2008) as described above.

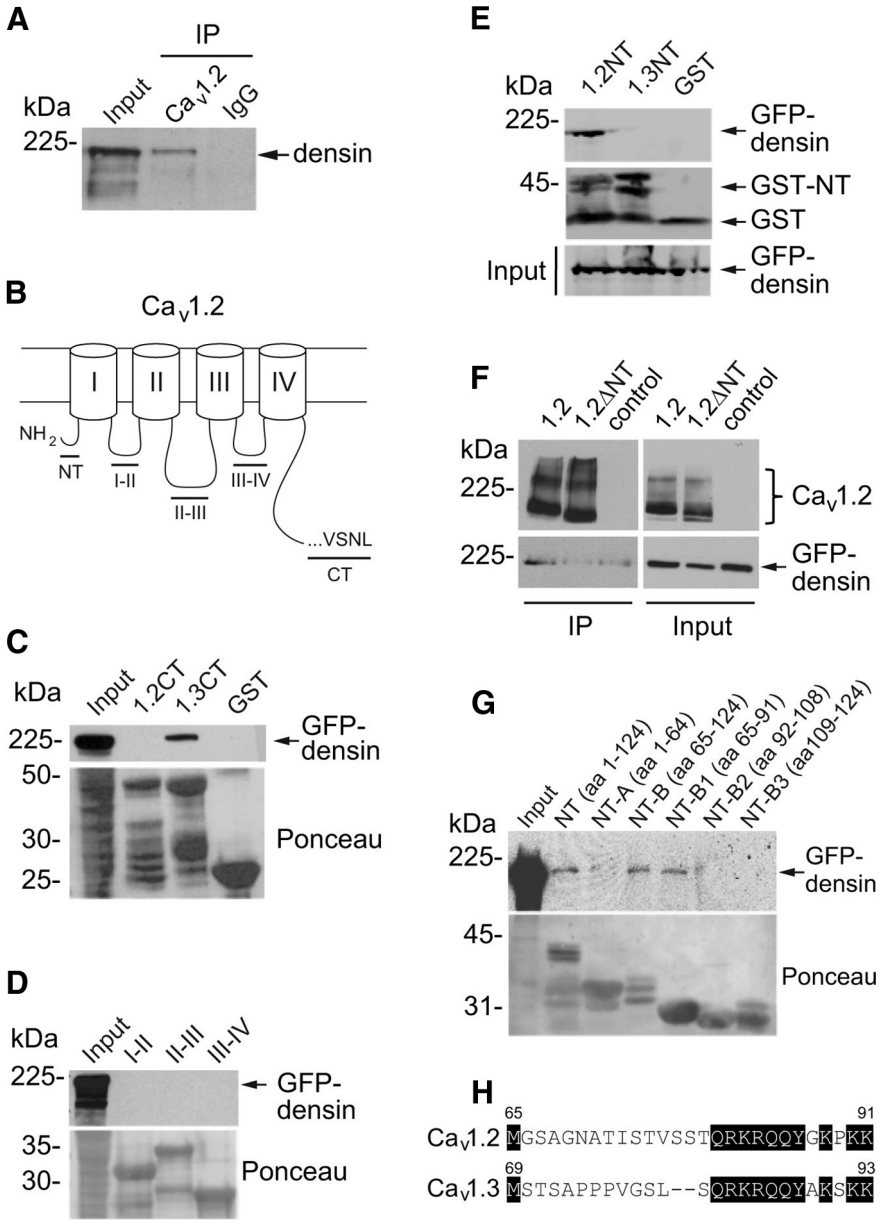

Figure 1. Densin interacts with $Ca_v1.2$ channels in the brain and binds to a site in the NT domain of $Ca_v1.2$. ***A***, Coimmunoprecipitation of densin with $Ca_v1.2$ antibodies but not rabbit control IgG in lysates of mouse prefrontal cortex. Western blotting was performed using a densin antibody. ***B***, Schematic of $Ca_v1.2$ α_1 subunit showing the NT domain, the C-terminal (CT) domain, and cytoplasmic loops (I–II, II–III, and III–IV). ***C–E***, Pull-down assays using GST-tagged cytoplasmic domains of $Ca_v1.2$. Input represents GFP-tagged densin in lysates of transfected HEK293T cells. ***C***, Densin binds to the CT of $Ca_v1.3$, but not that of $Ca_v1.2$. ***D***, Densin does not bind to the cytoplasmic loops of $Ca_v1.2$. ***E***, Densin binds to the NT of $Ca_v1.2$, but not that of $Ca_v1.3$. ***F***, Coimmunoprecipitation of GFP-densin with FLAG antibodies in HEK293T cells cotransfected with FLAG-tagged $Ca_v1.2$ (1.2), but not with $Ca_v1.2$ lacking the NT (1.2ΔNT) or control cells transfected with GFP-densin alone. ***G***, Same as in ***C–E*** except with GST-tagged fragments of the $Ca_v1.2$ NT. Amino acid numbers are indicated in parentheses. All blots shown are representative of at least three independent experiments. Input lanes represent 7–10% of starting material. ***H***, Sequence alignment of the B1 regions of $Ca_v1.2$ and $Ca_v1.3$. Conserved residues are shaded in black. Numbers indicate the amino acid residues.

Preparation of neuronal cultures. Low-density cultures of hippocampal neurons were prepared from BALB/c mice at embryonic day 18 as described previously (Obermair et al., 2004; Di Biase et al., 2011). Briefly, dissected hippocampi were dissociated by trypsin treatment and trituration. Neurons were plated on poly-L-lysine-coated glass coverslips in 60 mm culture dishes at a density of ~3500 cells/cm^2. After plating, cells were allowed to attach for 3–4 h before transferring the coverslips neuron-side down into a 60 mm culture dish with a glial feeder layer. Neurons and glial feeder layer were maintained in serum-free Neurobasal medium (Invitrogen) supplemented with Glutamax and B-27 supplements (Invitrogen). Ara-C (5 μM) was added 3 d after plating and, once a week, 1/3 of the medium was removed and replaced with fresh maintenance medium.

Cortical neuron cultures were prepared from postnatal day 0–1 mouse pups. The cerebral cortex was isolated in ice-cold dissection solution (0.1 mg/ml HBSS-containing sodium pyruvate, 0.1% glucose, and 10 mM HEPES, pH 7.3). The tissue was washed and digested for 13 min in the dissection solution containing trypsin (5 mg/ml) and DNase I (0.1 mg/ml) at room temperature. The trypsin was inactivated by two washes in prewarmed plating medium containing Eagle's basal medium (Thermo Fisher Scientific), fetal bovine serum (10%), w/v glucose (0.45%), sodium pyruvate (1 mM), glutamine (2 mM), and penicillin/streptomycin (100 μg/ml). The tissue was dissociated using polished Pasteur pipettes and the cells were pelleted at 185 × *g* for 13 min at 4°C. The cells were gently resuspended in prewarmed plating medium and plated on 18 mm glass coverslips coated with poly-D-lysine. Neurons were maintained in maintenance medium containing Neurobasal medium (Thermo Fisher Scientific), B27 (Thermo Fisher Scientific), glutamine (2 mM), and penicillin/streptomycin (100 μg/ml) at 37°C in a humidified atmosphere with 5% CO_2 for 12–16 d before experiments.

Analysis of cell surface $Ca_v1.2$ and densin localization in transfected hippocampal neurons. Expression plasmids were introduced into neurons at 6 d *in vitro* (DIV) using Lipofectamine 2000-mediated transfection (Invitrogen) as described previously (Obermair et al., 2004). For cotransfection of $Ca_v1.2$-HA + eGFP or $Ca_v1.2$-HA + eGFP + GFP-densin, 1.5 or 2.5 μg of total DNA was used at a molar ratio of 1:1 or 1:1:1, respectively. Cells were processed for immunostaining 12–13 d after transfection.

For surface staining of $Ca_v1.2$-HA, transfected neurons were incubated with anti-HA (Roche catalog #11867431001, RRID: AB_390919) for 20 min at 37°C. Coverslips were rinsed in HBSS and fixed with 4% paraformaldehyde for 10 min. After fixation, neurons were washed with PBS for 30 min, blocked with 5% goat serum for 30 min, and labeled with goat anti-rat Alexa Fluor 594 (1:4000, 1 h, Thermo Fisher Scientific catalog #A11007, RRID: AB_10561522). Coverslips were mounted in p-phenylenediamine glycerol to retard photobleaching (Flucher et al., 1993) and observed with an Axio Imager microscope (Carl Zeiss) using 63×, 1.4 numerical aperture oil-immersion objective lens. Images were recorded with cooled CCD camera (SPOT Imaging Solutions).

Fourteen-bit gray scale images of anti-HA (red channel) and eGFP (green channel) were acquired and analyzed as described previously (Di Biase et al., 2008; Di Biase et al., 2011; Stanika et al., 2016). Briefly, images were aligned and the eGFP image was used to select the regions of interest for measuring the area occupied by $Ca_v1.2$-HA clusters with MetaMorph software (Molecular Devices).

Electrophysiology. HEK293T cells were subjected to whole-cell patch-clamp recordings 48 h after transfection. For each experiment, control cells were recorded on the same day in parallel with experimental cells. The external solution contained the following (in mM): 150 Tris, 1

$MgCl_2$, and 10 $CaCl_2$ or $BaCl_2$. The internal solution contained the following (in mM): 140 *N*-methyl-D-glucamine, 10 HEPES, 2 $MgCl_2$, 2 Mg-ATP, and 5 EGTA. The pH of both solutions was adjusted to 7.3 with methanesulfonic acid. Electrode resistances were 6–8 MΩ in the bath solution and series resistance was ~6–8 MΩ compensated 70%. The holding voltage was −80 mV for transfected cells. Maximal gating charge was measured as the time integral of the gating current within 1.5–2 ms of a depolarizing step to the reversal potential (+70 mV) and tail current amplitudes were measured upon repolarization to −70 mV. Statistical analyses were as indicated.

For neuronal recordings, pyramidal neurons (12–16 DIV) were selected based on a pyramidal-shaped cell body and large proximal dendrites. The experimenter was blinded to mouse genotype before preparation of neuronal culture, recording, and data analysis. The external solution contained the following (in mM): 150 TEA-Cl, 5 $BaCl_2$, 10 HEPES, and 10 glucose, pH 7.4 with TEA-OH. The intracellular solution contained the following (in mM): 180 *N*-methyl-D-glucamine, 4 $MgCl_2$, 5 EGTA, 40 HEPES, 12 creatine-phosphate-Tris, 0.1 Leupeptin, 2 Na-ATP, and 0.4 Na-GTP, pH 7.3 with phosphoric acid. To isolate Ca_v1-mediated currents, external solution containing isradipine (5 μM; Tocris Bioscience) was applied by gravity perfusion. Currents were evoked by voltage ramps from −60 mV to +80 mV at 0.5 mV/ms from an initial holding potential of −60 mV.

Data were acquired with an EPC-9 amplifier and Patchmaster software (HEKA Elektronik) and analyzed using Igor Pro software (Wavemetrics). Statistical analysis was performed using SigmaPlot (Systat Software). Average data are presented as mean ± SEM. For current–density plots, peak current amplitudes were normalized to whole-cell capacitance. Current–voltage (*I–V*) relationships were fit with the following equation: $I = G(V - E)/\{1 + \exp[(V - V_{1/2})/k]\}$ where *G* is conductance, *V* is the test potential, *E* is the reversal potential, $V_{1/2}$ is the voltage for the half-maximal activation, and *k* is the slope factor.

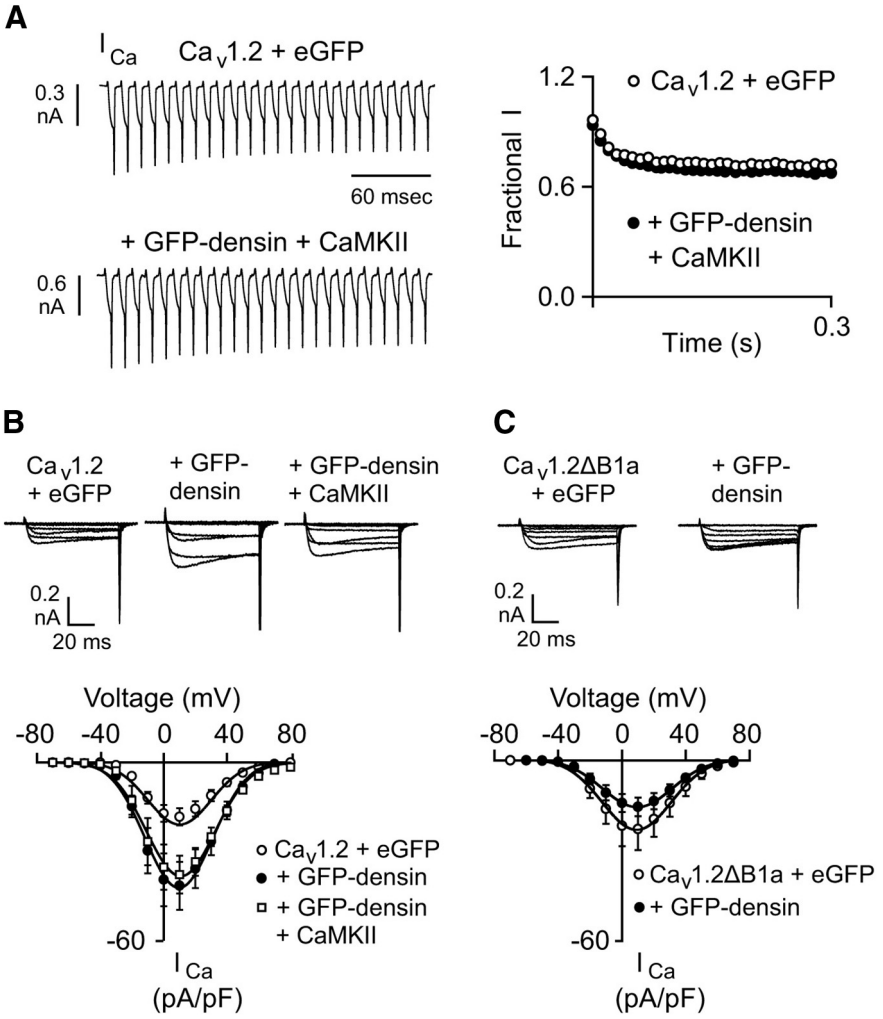

Figure 2. Densin does not cause CDF but increases current density of $Ca_v1.2$ in HEK293T cells. ***A***, I_{Ca} was evoked by 5 ms pulses from −80 to 10 mV at 100 Hz in cells transfected with $Ca_v1.2$ alone ($n = 13$) or cotransfected with densin and CaMKII ($n = 11$). Test current amplitudes were normalized to the first in the train (Fractional I) and plotted against time (right). ***B***, I_{Ca} was evoked by 50 ms depolarizations from −80 mV to various voltages and normalized to cell capacitance. Representative current traces and plots of current density against voltage are shown for cells transfected with $Ca_v1.2$ and: eGFP ($n = 13$), GFP-densin ($n = 15$), and GFP-densin + CaMKII ($n = 11$). ***C***, Same as in ***B*** except for I_{Ca} recorded in cells transfected with $Ca_v1.2\Delta B1a$ and eGFP ($n = 14$) or GFP-densin ($n = 14$).

Analyses of cell surface $Ca_v1.2$ protein levels in mouse brain. Biotinylation of cell surface proteins in brain slices were modified from methods described previously (Robertson et al., 2010). Wild-type (WT) and densin KO mice (3–6 weeks old, male) were deeply anesthetized with isoflurane (4–5%) and rapidly decapitated. The brain was removed and the prefrontal cortex was dissected and chilled in oxygenated solution containing the following (in mM): 210 sucrose, 20 NaCl, 2.5 KCl, 1 $MgCl_2$, and 1.2 $NaH_2PO_4 \cdot H_2O$ before sectioning. Coronal slices (300 μm) were collected using a vibratome (Electron Microscopy Science 5000 Oscillating Tissue Slicer) in artificial CSF (ACSF) containing the following (in mM): 125 NaCl, 2.5 KCl, 1.2 $NaH_2PO_4 \cdot H_2O$, 1 $MgCl_2$, and 2 $CaCl_2 \cdot H_2O$, oxygenated. To minimize cell damage, the highest oscillation speed and the lowest advance rate of the blade were chosen during slicing. The brain slices were immediately washed twice with ACSF before incubating with ACSF containing EZ-Link Sulfo-NHS-SS-Biotin (1 mg/ml; Thermo Fisher Scientific) for 45 min. The tissue was rinsed twice quickly and for two 10 min washes in ACSF. The reaction was quenched by washing twice for 20 min each with ACSF containing glycine before lysis in radioimmunoprecipitation assay (RIPA) buffer containing 25 mM Tris, 150 mM NaCl, 0.5% sodium deoxycholate, 0.1% SDS, 1% Triton X-100, and a mixture of protease inhibitors. Lysates were then centrifuged at 12,000 × *g* for 30 min at 4°C. Biotinylated proteins were isolated on streptavidin beads (Thermo Fisher Scientific) overnight at 4°C with rotation. Beads were washed 3 times with RIPA buffer (0.1% Triton X-100) and biotinylated proteins were eluted in SDS-PAGE sample loading buffer at 90°C for 10 min. Western blotting was with antibodies against $Ca_v1.2$, Na^+/K^+ ATPase (1:3000, Developmental Studies Hybridoma Bank catalog #a6F RRID:AB_2314847) and GAPDH (1:10000, Abcam catalog #ab8245 RRID:AB_2107448).

Phosphorylated CREB assays. Cortical neurons (12–16 DIV) from WT or densin KO mice were incubated in maintenance medium containing 0.5 μM tetrodotoxin (TTX; Tocris Bioscience), 10 μM 6-cyano-7-nitroquinoxaline-2,3-dione (CNQX; Tocris Bioscience), and 10 μM D-(−)-2-amino-5-phosphonopentanoic acid (APV; Tocris Bioscience) at 37°C, 5% CO_2, for 4 h. Cells were exposed to Tyrode's solution containing the following (in mM): 150 NaCl, 2 $MgCl_2$, 2 $CaCl_2$, 10 HEPES, and 10 glucose, pH 7.3, and the following (in μM): 0.5 TTX, 10 CNQX, and 10 APV, plus either 5 or 40 mM KCl for 3 min, and immediately fixed in solution containing paraformaldehyde (4%), sucrose (4%), and EGTA (20 mM) at room temperature for 10 min. Cells were permeabilized in PBS with Triton X-100 (0.1%) for 10 min and blocked with normal goat serum (10%) in PBS for 1 h. Primary antibod-

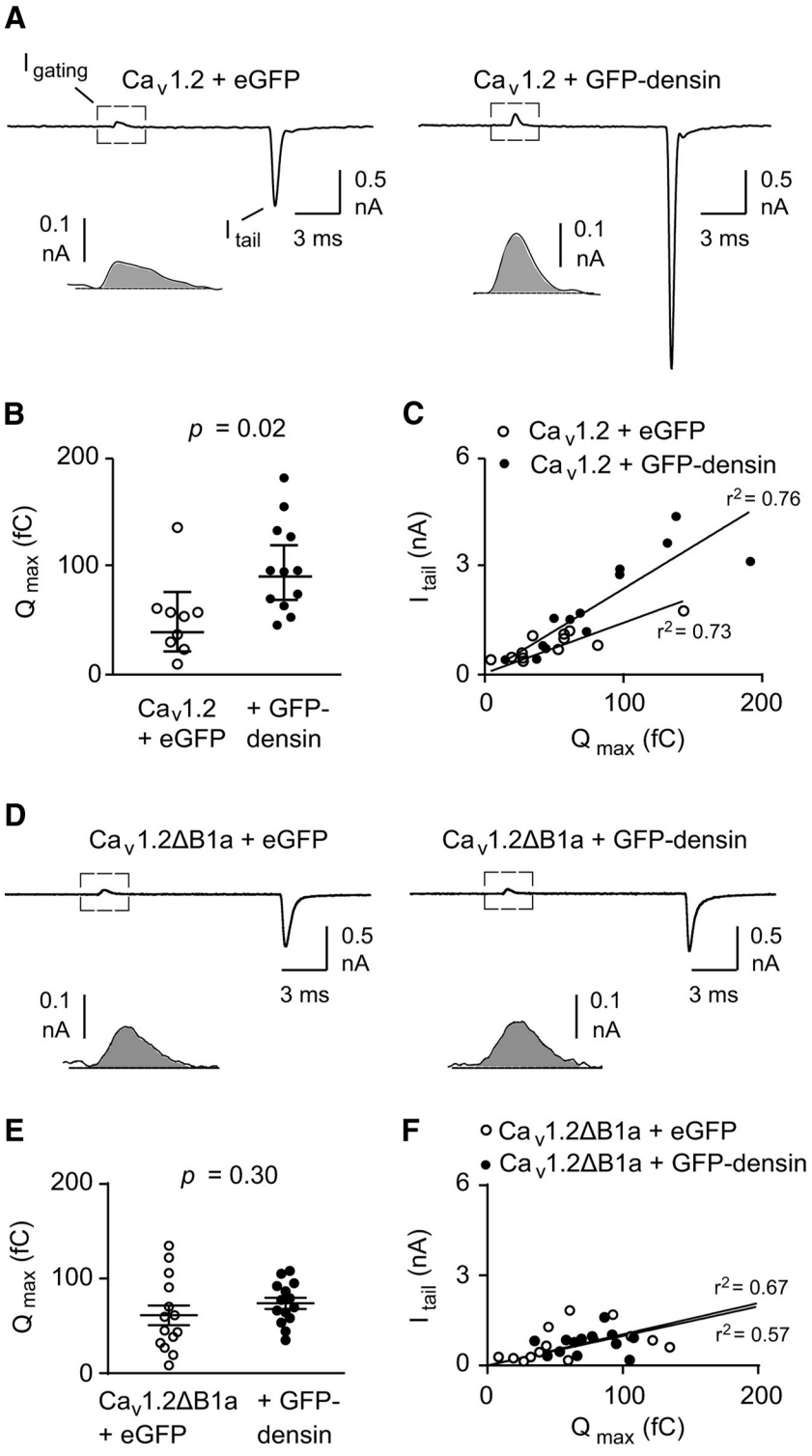

Figure 3. Densin increases the number of functional $Ca_v1.2$ channels and their relative open probability. ***A***, Representative traces showing I_{gating} and I_{tail} measured at the reversal potential (+70 mV). Inset shows outward gating current on expanded timescale. Shaded area indicates Q_{max}. ***B***, ***C***, Dot plot of Q_{max} (***B***) and I_{tail} versus Q_{max} (***C***) in cells cotransfected with $Ca_v1.2$ and eGFP ($n = 9$) or GFP-densin ($n = 12$). The fit by linear regression and coefficient of determination (r^2) are shown. ***D–F***, Same as in ***A–C*** except in cells transfected with $Ca_v1.2\Delta B1a$ and eGFP ($n = 14$) or GFP-densin ($n = 14$). *p*-values were determined by *t* test.

ies were rabbit anti-phosphorylated CREB (pCREB) (1:300; Cell Signaling Technology catalog #9198S, RRID: AB_390802); mouse anti-CaMKIIα (1:2000, Thermo Fisher Scientific catalog #MA1-048, RRID: AB_325403); mouse anti-NeuN (1:100, Millipore catalog #MAB377, RRID: AB_2298772) and were diluted in PBS, added to the coverslips, and incubated overnight at 4°C. The cells were then washed 3 times with PBS and incubated in anti-rabbit Alexa Fluor 488 (Thermo Fisher Scientific catalog #A31565, RRID: AB_10373124) and goat anti-mouse Alexa Fluor 568 (1:500; Thermo Fisher Scientific catalog #A-21134, RRID: AB_2535773) for 1 h at room temperature. After additional washing, cells were incubated in Hoechst 33342 (1 μg/ml) in distilled water for 15 min before mounting on microscope slides. The cells were visualized with a 60× oil-immersion objective on a confocal microscope (Fluoview 1000; Olympus). The level of pCREB fluorescence was quantified in confocal images analyzed in ImageJ software. The nuclear marker Hoechst and anti-NeuN staining were used to identify the region of interest over each neuron. The region adjacent to the neuron was regarded as background. Mean pixel intensity for pCREB immunofluorescence was measured in the region of interest and the background level was subtracted. Genotypes of animals were revealed after the quantification.

Trafficking assays. For endocytosis assays, transfected HEK293T cells were washed twice with Dulbecco's PBS with $MgCl_2$ and $CaCl_2$ ($DPBS^{2+}$; Thermo Fisher Scientific) 48 h after transfection. Live cells were incubated with mouse anti-HA antibodies (1:100, Sigma-Aldrich catalog #11583816001, RRID: AB_514505) at 37°C for 15 min. After washing 3 times with $DPBS^{2+}$ at room temperature, the cells were maintained at 37°C for varying periods to allow for channel internalization before fixing in ice-cold paraformaldehyde (4%) in $DPBS^{2+}$ for 10 min. Cells were then blocked with normal goat serum (10%), followed by incubating with anti-$Ca_v1.2$ antibodies overnight and the corresponding Alexa Fluor secondary antibodies and washes as described above. Images were taken using 60× oil-immersion objectives with a constant acquisition setting on a confocal microscope (Fluoview 1000; Olympus). The cell surface HA fluorescence in $Ca_v1.2$-positive cells was quantified in ImageJ software using the freehand brush tool to trace the membrane region stained by anti-HA antibodies manually for measuring the cell surface fluorescence density.

For forward trafficking, cells transfected with $Ca_v1.2$-SNAP were incubated with BG-Block (2 μM; New England BioLabs catalog #S9106S) at 37°C for 30 min to block existing channels. The cells were then washed 3 times and incubated in complete medium for varying durations before incubating with TMR-STAR (2 μM; New England BioLabs catalog #S9105S) at 37°C for 25 min to label newly synthesized channels. After washing with complete medium, cells were fixed for 10 min at 4°C in paraformaldehyde (4%), washed in $DPBS^{2+}$, and blocked in $DPBS^{2+}$ containing goat serum (10%). Cells were then incubated with anti-HA antibodies for cell surface labeling and the appropriate Alexa Fluor secondary antibodies. Cell surface TMR-STAR fluorescence was quantified in ImageJ as described above. Whole-cell fluorescence densities were quantified using freehand selection, omitting the signal intensity from adjacent areas. The background fluorescence density in each channel was also taken from the same image and subtracted from the signal density. Data were acquired and analyzed without prior knowledge of protein expression profiles.

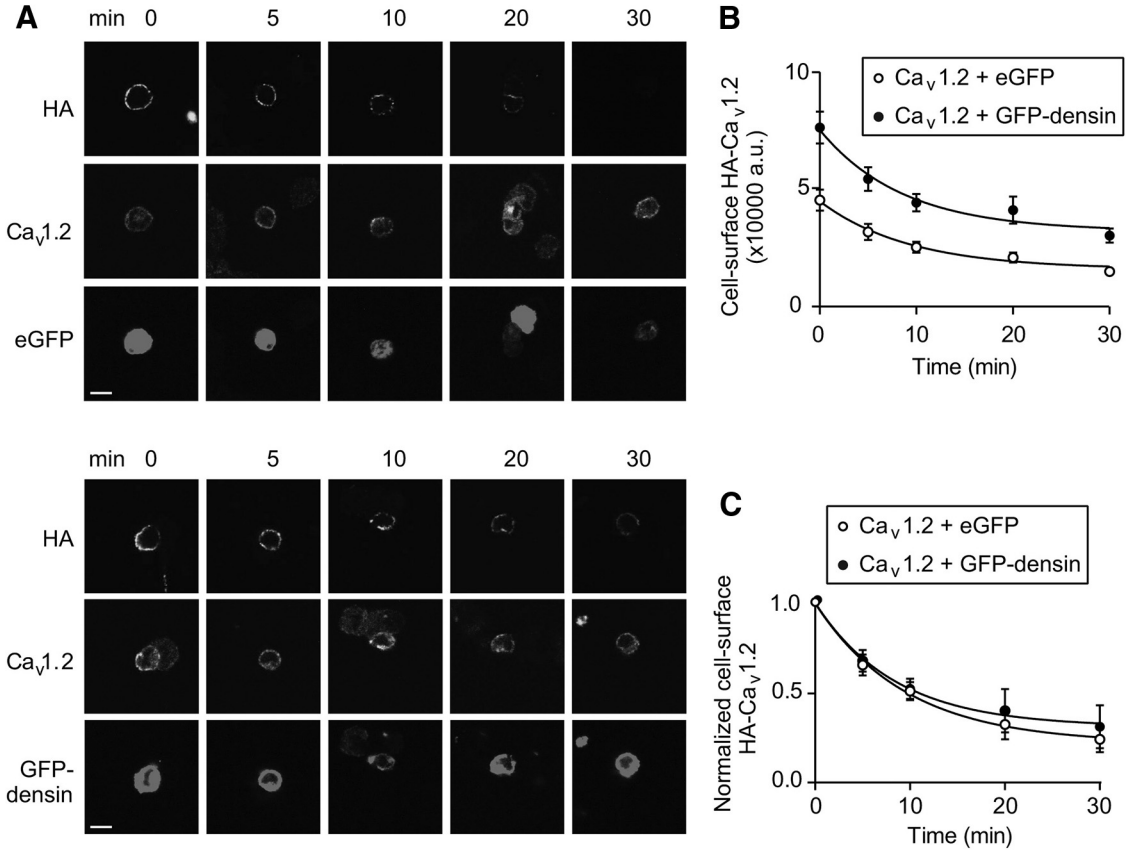

Figure 4. Densin does not affect internalization of $Ca_v1.2$ in transfected HEK293T cells. ***A***, Cells expressing $Ca_v1.2$-HA and eGFP (top) or GFP-densin (bottom) were incubated with HA antibodies to label cell surface channels and incubated for the indicated times (in minutes) to allow for channel internalization. The cells were then fixed and processed with $Ca_v1.2$ antibodies to label total channel protein. Scale bars, 10 μm. ***B***, Cell surface HA fluorescence (arbitrary units, a.u.) was plotted against internalization time. Results are representative of three independent experiments. ***C***, Same as ***B*** but HA intensity was normalized to that at time = 0 min. Smooth line represents fit with a single exponential equation.

Results

Densin interacts differentially with and regulates $Ca_v1.2$ and $Ca_v1.3$

To determine whether densin is a physiological partner of $Ca_v1.2$ *in vivo*, we tested whether the two proteins form a complex in mouse brain. Antibodies that specifically recognize $Ca_v1.2$ (Tippens et al., 2008) were used to immunoprecipitate proteins from lysates of the mouse prefrontal cortex. Western blotting with densin antibodies revealed that densin coimmunoprecipitated with $Ca_v1.2$ antibodies, but not with control IgG (Fig. 1*A*). Because densin binds to the PDZ-binding site at the C terminus of $Ca_v1.3$ (Jenkins et al., 2010), we hypothesized that densin would similarly bind to the corresponding region of $Ca_v1.2$. In pull-down assays, GST fusion proteins containing the distal C terminus of $Ca_v1.2$ did not bind to GFP-densin despite interacting with the same region of $Ca_v1.3$ (Fig. 1*B*,*C*). GFP-densin also did not bind to the cytoplasmic loops of $Ca_v1.2$ (Fig. 1*D*). However, specific binding of GFP-densin was found for the N-terminal (NT) domain of $Ca_v1.2$ but not $Ca_v1.3$ (Fig. 1*E*). Moreover, deletion of the NT domain prevented coimmunoprecipitation of GFP-densin with $Ca_v1.2$ ($Ca_v1.2\Delta$NT; Fig. 1*F*). Using GST-tagged fragments of the $Ca_v1.2$ NT, we found that GFP-densin bound specifically to proteins containing aa 65–91 (Fig. 1*G*). Because aa 77–91 are largely conserved in $Ca_v1.3$ (Fig. 1*H*), the major determinants for densin binding to the $Ca_v1.2$ NT appear to reside between aa 65 and 76.

To elucidate the functional impact of densin on $Ca_v1.2$, we turned to an electrophysiological protocol we used previously to uncover the modulatory effects of densin on $Ca_v1.3$. When cotransfected with densin and its interacting protein, CaMKII (Strack et al., 2000; Walikonis et al., 2001), $Ca_v1.3$ channels undergo Ca^{2+}-dependent facilitation during repetitive depolarizations (Jenkins et al., 2010). Although there was no effect of densin and CaMKII on $Ca_v1.2$ Ca^{2+} currents (I_{Ca}) with this protocol (Fig. 2*A*), *I–V* relationships revealed significantly greater current densities in cells cotransfected with GFP-densin and CaMKII than in control cells (at +10 mV, 38.0 ± 6.4 pA/pF for $Ca_v1.2$ + GFP-densin + CaMKII, $n = 13$, vs 20.7 ± 2.8 pA/pF for $Ca_v1.2$ + eGFP, $n = 14$, $p = 0.02$ by t test; Fig. 2*B*). This effect did not require CaMKII because it was reproduced in cells cotransfected with only $Ca_v1.2$ and GFP-densin (Fig. 2*B*). Densin did not augment I_{Ca} in cells cotransfected with channels lacking the NT aa 65–76 ($Ca_v1.2\Delta$B1a) comprising the densin-binding site (at +10 mV, 15.4 ± 2.8 pA/pF for $Ca_v1.2\Delta$B1a + GFP-densin, $n = 14$, vs 22.5 ± 5.6 pA/pF for $Ca_v1.2\Delta$B1a + eGFP, $n = 14$, $p = 0.29$; Fig. 2*C*). These results indicate that densin binding to $Ca_v1.2$ is required for the enhanced current density in cells cotransfected with GFP-densin.

GFP-densin could increase I_{Ca} by increasing the number of $Ca_v1.2$ channels and/or their activity in the cell membrane. To pinpoint the underlying mechanism, we measured the gating current upon depolarization to the reversal potential (I_{gating}) and the tail current (I_{tail}) evoked by repolarization to the holding voltage (Fig. 3*A*). The time integral of I_{gating} (Q_{max}) estimates the number of channels in the cell membrane and the ratio of I_{tail} and Q_{max} reflects the relative channel open probability (Wei et al.,

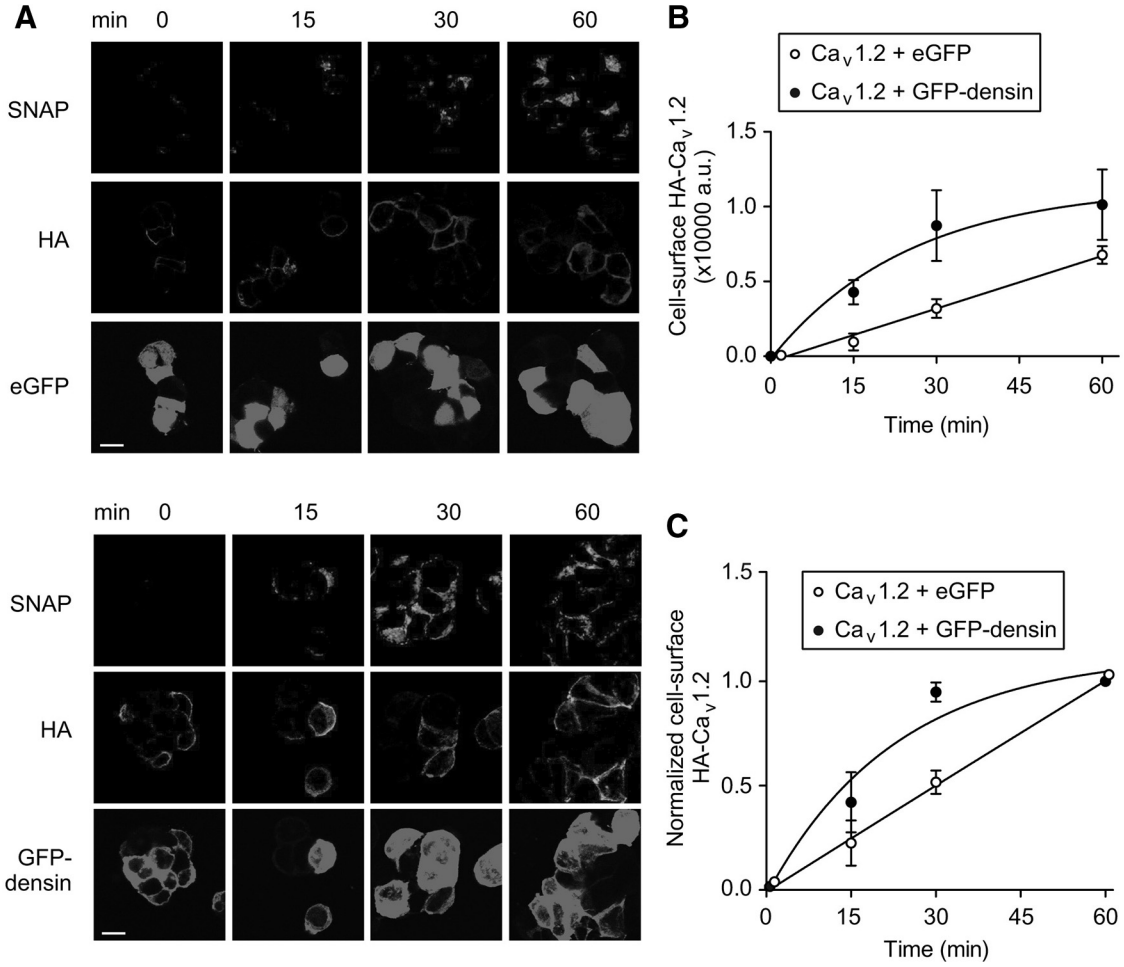

Figure 5. Densin accelerates the forward trafficking of $Ca_v1.2$ in transfected HEK293T cells. ***A***, Cells expressing $Ca_v1.2$-HA-SNAP and eGFP (top) or GFP-densin (bottom) were processed for TMR-STAR labeling of newly synthesized channels (see Materials and Methods). After incubation for the indicated times to allow forward trafficking of channels, cells were subjected to labeling with HA antibodies to mark cell surface channels. Scale bars, 10 μm. ***B***, Cell surface TMR-STAR fluorescence (arbitrary units, a.u.) was plotted against forward trafficking time. Results are representative of three independent experiments. ***C***, Same as ***B*** but TMR-STAR signal was normalized to that at time = 60 min. Smooth line represents fit with a single exponential equation.

1994; Takahashi et al., 2004). Cotransfection of GFP-densin caused a significant increase in Q_{max} (50.8 ± 14.1 fC for $Ca_v1.2$ + eGFP, $n = 9$ vs 94.6 ± 17.5 fC for $Ca_v1.2$ + GFP-densin, $n = 13$, $p = 0.02$ by t test; Fig. 3*B*). The slope of the I_{tail}–Q_{max} relationship was steeper (~2-fold; Fig. 3*C*) in cells cotransfected with GFP-densin compared with cells transfected with $Ca_v1.2$ and eGFP. Therefore, densin enhances the number of functional channels as well as their open probability. To determine whether the effect of densin requires interaction with the channel, we deleted the densin-binding sequence within the NT ($Ca_v1.2\Delta B1a$ + eGFP). In cells transfected with this construct, GFP-densin did not affect Q_{max} (61.2.0 ± 10.4 fC for $Ca_v1.2\Delta B1a$ + eGFP, $n = 14$ vs 73.9 ± 5.9 fC for $Ca_v1.2\Delta B1a$ + GFP-densin, $n = 14$, $p = 0.30$ by t test; Fig. 3*D*,*E*) or the I_{tail}–Q_{max} relationship (Fig. 3*F*). Similar results were obtained for $Ca_v1.2\Delta NT$ (data not shown). These results demonstrate that the interaction of densin with $Ca_v1.2$ is required for facilitation of channel function by densin.

Densin promotes the forward trafficking of $Ca_v1.2$ channels

The effect of densin on the number of $Ca_v1.2$ channels could result from a larger amount of $Ca_v1.2$ protein in the plasma membrane either from reduced endocytosis and/or enhanced forward trafficking. To test this, we used $Ca_v1.2$ channels tagged with an external HA epitope ($Ca_v1.2$-HA; Altier et al., 2002) such that cell surface levels of channel could be measured by labeling with HA antibodies in living cells. After antibody labeling, HEK293T cells cotransfected with $Ca_v1.2$-HA and eGFP or GFP-densin were incubated in fresh medium for varying durations to allow for channel internalization (Fig. 4*A*). The level of cell surface $Ca_v1.2$-HA was significantly greater in cells cotransfected with GFP-densin than with eGFP at all time points ($p < 0.0001$ by ANOVA; Fig. 4*B*). However, exponential fits of the data normalized to $Ca_v1.2$ HA staining at the start of the experiment (time = 0 min) indicated no effect of densin on the speed of internalization of $Ca_v1.2$-HA ($\tau = 8.4 \pm 0.7$ min for GFP-densin, $n = 62$ cells, vs $\tau = 9.5 \pm 0.8$ min for eGFP, $n = 60$ cells, $p = 0.22$; Fig. 4*C*). These results confirm that densin increases the cell surface density of $Ca_v1.2$ channels, but not by inhibiting their endocytosis.

To determine whether densin enhances the trafficking of $Ca_v1.2$ to the cell surface, we generated $Ca_v1.2$ constructs containing the SNAP tag, an engineered variant of the DNA repair protein O^6-alkylguanine-DNA-alkyltransferase that uses benzylguanine as a substrate (Keppler et al., 2004). SNAP-tagged $Ca_v1.2$-HA ($Ca_v1.2$-HA-SNAP) was cotransfected with eGFP or GFP-densin in HEK293T cells that were incubated first with benzylguanine to block existing channels. Subsequent incubation of the cells at 37°C for varying durations allowed for synthesis of new, unlabeled channels that were identified with a cell-permeant fluorescent derivative of

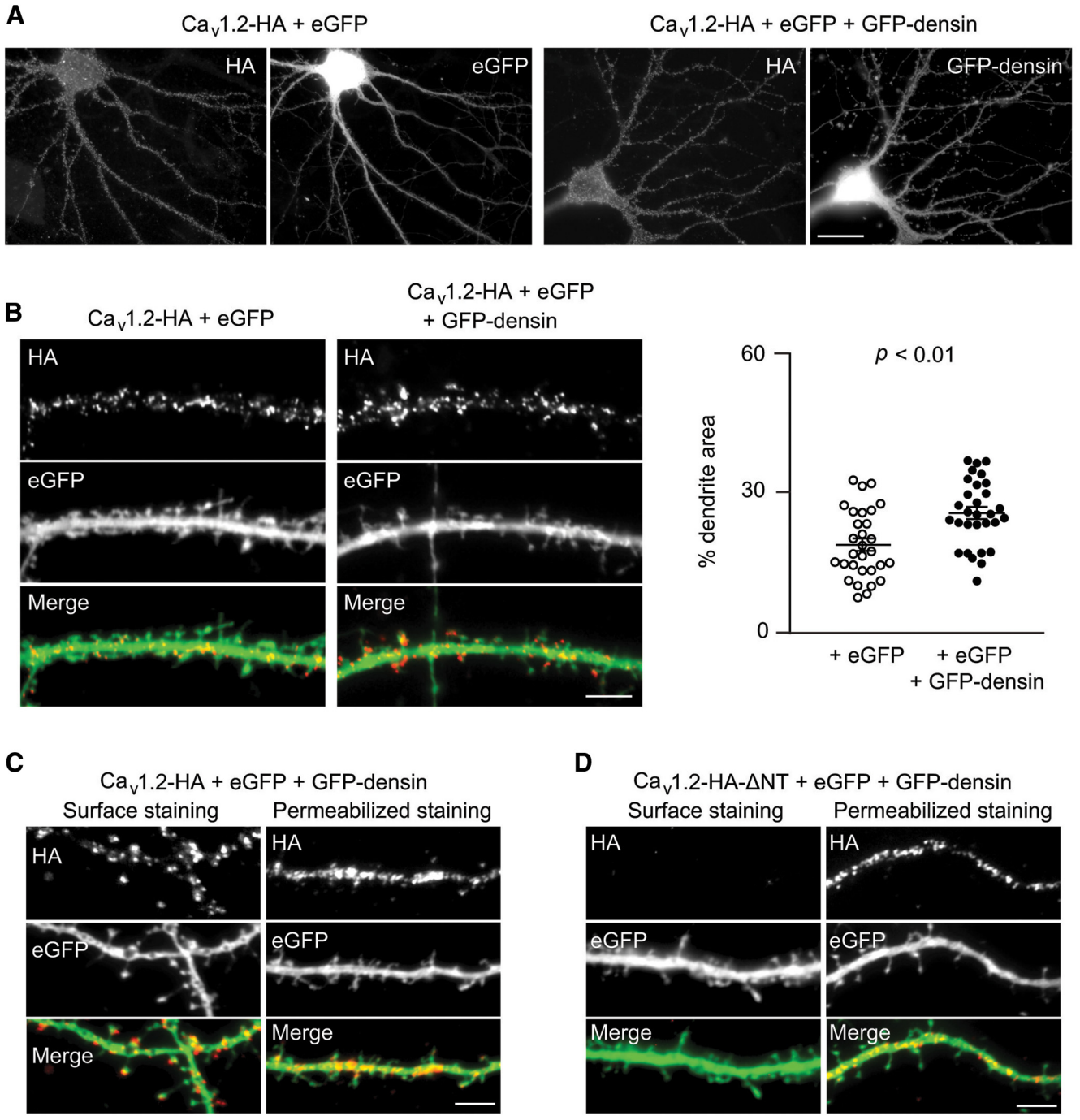

Figure 6. GFP-densin increases the cell surface levels of dendritic $Ca_v1.2$ channels in neurons. ***A***, Mouse hippocampal neurons were transfected with $Ca_v1.2$-HA + eGFP together with or without GFP-densin and subjected to live labeling with HA antibodies to mark cell surface channels. Representative fluorescent images are shown. Scale bar, 20 μm. ***B***, Left, Dendrites of neurons transfected as in ***A*** shown at higher magnification. Scale bar, 5 μm. Data are representative of at least two independent experiments (number of dendrites analyzed per experiment: 15). Right, Quantification of cell surface $Ca_v1.2$-HA in hippocampal neurons expressed as the percentage of the dendritic area (defined by eGFP fluorescence) occupied by HA fluorescence. Statistical significance was determined by Student's *t* test. ***C***, ***D***, Dendrites of neurons transfected with eGFP, GFP-densin, and $Ca_v1.2$-HA (***C***) or $Ca_v1.2$-HA-ΔNT (***D***). Neurons were subjected to live cell staining with HA antibodies (left) or HA-labeling for total channels after permeabilization (right). Scale bars, 5 μm.

benzylguanine (TMR-STAR; Fig. 5*A*). The cells were then processed for live labeling with HA antibodies and colocalized TMR-STAR and HA fluorescence was used to estimate the density of cell surface $Ca_v1.2$ channels. As in the endocytosis experiments, cotransfection with GFP-densin increased the amount of cell surface channels at most time points (Fig. 5*B*). When normalized to the last time point (60 min), the maximal density of cell surface HA-$Ca_v1.2$ was achieved within 30 min in cells cotransfected with GFP-densin compared with 1 h for cells cotransfected with eGFP (Fig. 5*C*). Therefore, densin increases the cell surface density of $Ca_v1.2$ channels by enhancing their trafficking to, rather than decreasing their removal from, the plasma membrane.

Densin increases the cell surface levels of $Ca_v1.2$ in neurons

In neurons, $Ca_v1.2$ and densin are primarily localized in somatodendritic regions, particularly in dendritic spines (Apperson et al., 1996;

Obermair et al., 2004; Tippens et al., 2008). To determine whether densin regulates the trafficking of $Ca_v1.2$ in neurons, we analyzed the distribution of cell surface $Ca_v1.2$-HA cotransfected with eGFP or GFP-densin in dendrites of hippocampal neurons in culture under nonpermeabilized conditions. We chose this approach rather than immunolabeling endogenously expressed $Ca_v1.2$ because $Ca_v1.2$ antibodies that are currently available recognize intracellular epitopes; the detergent permeabilization required for immunofluorescent detection would not restrict analysis to cell surface channels. Because densin is primarily localized at synapses of hippocampal neurons (Carlisle et al., 2011; Stanika et al., 2016), control and experimental groups were cotransfected with eGFP because the diffuse localization of eGFP in dendrites and dendritic spines facilitates the selection of dendritic regions for the analysis of cell surface channel clusters (Obermair et al., 2004). Consistent with previous studies (Obermair et al., 2004), punctate labeling for cell surface $Ca_v1.2$-HA channels was evident in the soma and dendrites. This distribution of $Ca_v1.2$-HA was qualitatively similar in neurons transfected with GFP-densin and eGFP alone (Fig. 6*A*). Consistent with our results in transfected HEK293T cells (Figs. 4, 5), quantitative analyses revealed that cotransfection with GFP-densin increased the dendritic area covered by cell surface clusters of $Ca_v1.2$-HA channels (Fig. 6*B*).

To verify that densin binding to $Ca_v1.2$ was required for this effect, we initially analyzed neurons transfected with GFP-densin and $Ca_v1.2$-HA-ΔB1a, which does not interact functionally with densin in HEK293T cells (Figs. 2*C*, 3*D–F*). However, $Ca_v1.2$-HA-ΔB1a did not express at high levels in neurons (data not shown). Therefore, we turned to $Ca_v1.2$-HA-ΔNT, which lacks the entire NT domain and also does not interact with densin (Fig. 1*F*). Total levels of $Ca_v1.2$-HA-ΔNT measured by HA labeling under permeabilized conditions were not different from those of WT $Ca_v1.2$-HA, but we could not detect $Ca_v1.2$-HA-ΔNT at the cell surface when coexpressed with GFP-densin (Fig. 6*C*,*D*). Although we cannot rule out the possibility that the NT has additional roles in promoting insertion of $Ca_v1.2$ in the dendritic membrane, our results are consistent with the importance of the densin–$Ca_v1.2$ interaction in determining the postsynaptic levels of $Ca_v1.2$ in neurons.

Ca_v1 current density and signaling to the nucleus are weakened in neurons from densin KO mice

If densin supports the cell surface levels of $Ca_v1.2$ in neurons, then genetic inactivation of densin should cause a reduction in Ca_v1 current density and signaling in neurons. To test this, we used densin KO mice that were characterized previously (Carlisle et al., 2011). In whole-cell patch-clamp recordings, voltage ramps were used to evoke Ba^{2+} currents (I_{Ba}) in cortical neuron cultures obtained from WT and densin KO mice. Because multiple classes of Ca_v channels are expressed in these neurons (Lorenzon and Foehring, 1995), we isolated Ca_v1 currents pharmacologically by recording currents before and after bath perfusion of the Ca_v1 antagonist isradipine. Because $Ca_v1.2$ channels account for ~80–90% of Ca_v1 channels in the brain (Sinnegger-Brauns et al., 2004), this strategy should largely reflect $Ca_v1.2$-mediated I_{Ba}. Using the isradipine-sensitive current as a measure of the Ca_v1 current, Ca_v1 channels accounted for ~40% of peak I_{Ba}, which is similar to that reported in rat neocortical neurons (Lorenzon and Foehring, 1995). In recordings obtained from 3 separate neuronal cultures, the fractional Ca_v1 current was significantly greater (~2-fold) in neurons from WT mice (0.42 ± 0.07; $n = 8$ neurons) than from densin KO mice (0.22 ± 0.05, $n = 8$ neurons, $p < 0.02$; Fig. 7*A*,*B*).

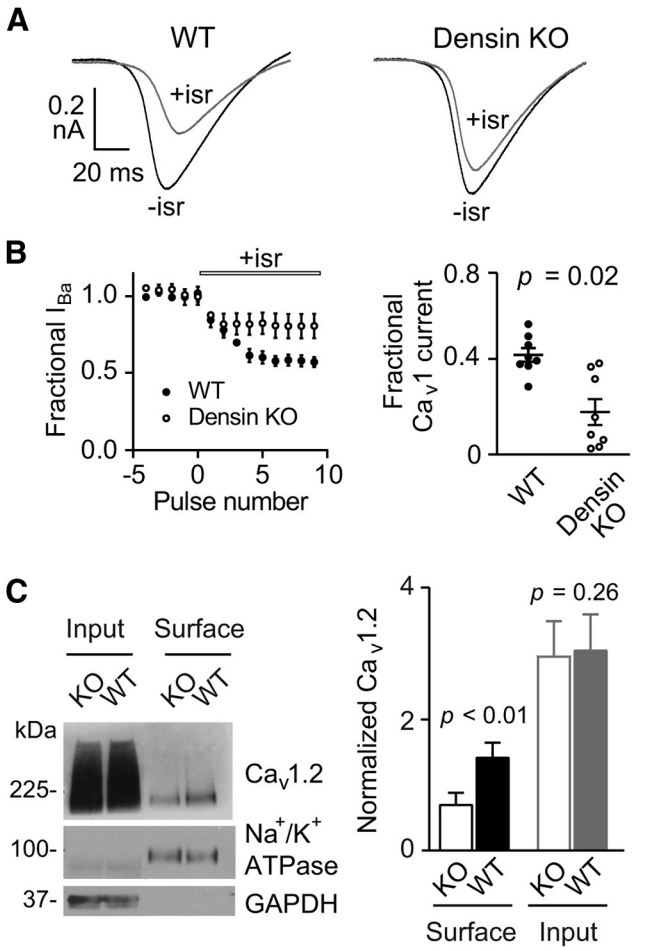

Figure 7. Ca_v1 currents and cell surface $Ca_v1.2$ protein levels are reduced in cortical neurons from densin KO mice. ***A***, I_{Ba} was evoked by voltage ramps from −60 to +80 mV (0.5 ms/mV) from a holding voltage of −60 mV in cortical neurons from WT ($n = 8$ cells from 3 mice) and densin KO ($n = 8$ from 3 mice) mice before (−isr) and after (+isr) bath application of isradipine (5 μM). ***B***, Measurement of the Ca_v1-mediated current. Left, Peak currents for data collected as in ***A*** were plotted for voltage ramps evoked every minute before and after application of isradipine. Right, Fractional Ca_v1 current represents the fraction of the total I_{Ba} that was blocked by isradipine. Statistical significance was determined by Student's *t* test. ***C***, Biotinylated cell surface proteins in prefrontal cortex of WT and densin KO mice were isolated on streptavidin agarose and subjected to Western blotting. Left, Representative Western blot probed with antibodies against $Ca_v1.2$, Na^+/K^+ ATPase, and GAPDH. Lanes represent biotinylated proteins before (input; ~10% of total amount used for pull-down) or after streptavidin pull-down (surface). Results are representative of four independent experiments, with one WT and one densin KO littermate used per experiment. Right, Densitometric analysis of biotinylated cell surface $Ca_v1.2$ channels. Signals corresponding to $Ca_v1.2$ were normalized to that for Na^+/K^+ ATPase (surface) or GAPDH (input). Results are from four independent experiments. Statistical significance was determined by Student's *t* test.

Although these results were consistent with a role for densin in enhancing the cell surface density of $Ca_v1.2$ channels, upregulation of non-Ca_v1 channels may have contributed to the decrease in the isradipine-sensitive current in densin KO neurons. Moreover, at the concentration used in our experiments, isradipine (5 μM) inhibits both $Ca_v1.2$ and $Ca_v1.3$ (Koschak et al., 2001). To confirm that decreased cell surface levels of $Ca_v1.2$ could explain the loss of Ca_v1 currents in densin KO neurons, we isolated cell surface proteins by biotinylation in brain slices and purification on streptavidin agarose followed by Western blotting with $Ca_v1.2$ antibodies. Although there was no difference in total $Ca_v1.2$ protein levels, there was ~50% less cell surface $Ca_v1.2$ in densin KO than in WT brain slices (Fig. 7*C*). This reduction is similar to, and

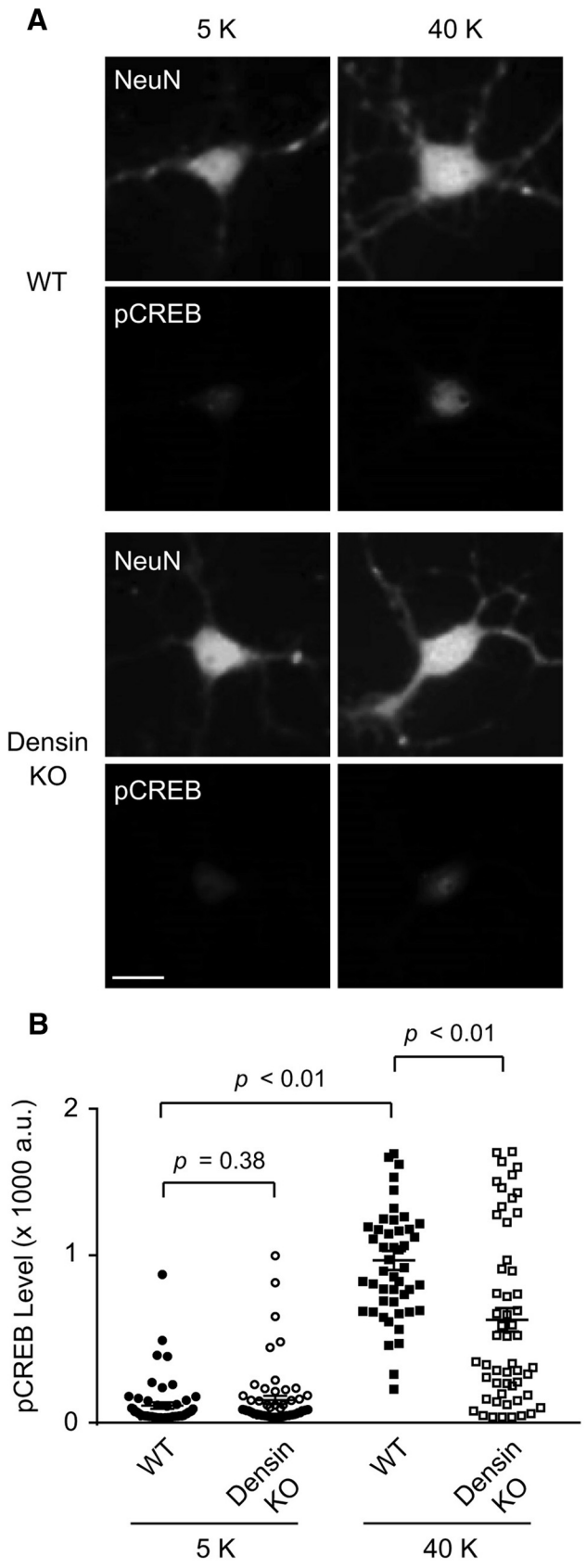

Figure 8. Excitation–transcription coupling is reduced in densin KO neurons. ***A***, Epifluorescence images of cortical neurons from WT and densin KO mice exposed to 5 or 40 mM K^+ for 3 min and processing for double-label immunofluorescence with antibodies against pCREB and the neuronal marker, NeuN. Images are representative of three independent experiments. ***B***, Quantification of the intensity of pCREB fluorescence (arbitrary units, a.u.) in WT and densin KO cortical neurons ($n = 50–58$ neurons per condition from three different sets of cultures). Statistical significance was determined by Student's *t* test.

thus may account for, the decrease in the Ca_v1 current in densin KO neurons (Fig. 7*A*,*B*). These results confirm that densin is required to support the cell surface density of $Ca_v1.2$ channels in the brain.

Activation of postsynaptic Ca_v1 channels promotes local Ca^{2+} signaling events that support activity-dependent gene transcription through phosphorylation of CREB (Wheeler et al., 2012), a transcription factor involved in synaptic plasticity and learning and memory (Deisseroth et al., 2003). If densin controls the number of postsynaptic $Ca_v1.2$ channels, then depolarization-induced levels of phosphorylated CREB (pCREB) should be reduced in densin KO neurons. To test this prediction, we fixed and immunolabeled neurons with antibodies recognizing pCREB after depolarization with solution containing 40 mM K^+, which strongly activates Ca_v1-mediated CREB phosphorylation (Wheeler et al., 2012). Although pCREB levels were not different between genotypes under basal conditions (i.e., with 5 mM K^+), the net increase in pCREB upon depolarization was significantly less in neurons from densin KO compared with WT mice (Fig. 8). We conclude that densin promotes excitation–transcription coupling in neurons, likely through enhancing the cell surface levels of postsynaptic $Ca_v1.2$ channels.

Discussion

Our study provides new insights into the role of densin in regulating neuronal Ca^{2+} signaling. First, in contrast to its interaction with the C-terminal domain of $Ca_v1.3$, densin binds to the NT of $Ca_v1.2$ and increases the cell surface levels of $Ca_v1.2$ by promoting its forward trafficking in transfected cells. Second, densin supports the postsynaptic levels of $Ca_v1.2$ in neurons, which are significantly reduced in the absence of densin. Finally, densin is required for robust Ca_v1-mediated excitation-transcription coupling in neurons. These effects of densin may contribute to the role of $Ca_v1.2$ in synaptic plasticity and spatial memory, processes that are disrupted in densin KO mice (Carlisle et al., 2011). In addition to regulating Ca^{2+} and CaMKII-dependent facilitation $Ca_v1.3$ (Jenkins et al., 2010), densin also regulates the clustering of heterologously expressed $Ca_v1.3$ channels in dendrites and the stability of dendritic spines in hippocampal neurons in culture (Stanika et al., 2016). Together with these findings, our results reveal densin as a multifunctional regulator of neuronal Ca_v1 channels.

The inability of densin to bind to the C-terminal domain of $Ca_v1.2$ may seem unexpected given that this region contains a type 1 PDZ-binding sequence similar to that which binds densin in $Ca_v1.3$ (Jenkins et al., 2010). However, there appears to be some selectivity with which PDZ-domains associate with the Ca_v1 C termini. For example, the PDZ domains of Erbin and Shank interact with the C termini of $Ca_v1.3$, but not $Ca_v1.2$ (Zhang et al., 2005; Calin-Jageman et al., 2007). Although deletion of the $Ca_v1.2$ PDZ-binding site does not affect $Ca_v1.2$ trafficking in neurons (Di Biase et al., 2008) or cardiac myocytes (Yang et al., 2015), deletions within the NT domain increase the cell surface density and maximal open probability of $Ca_v1.2$ in *Xenopus* oocytes (Wei et al., 1996; Kanevsky and Dascal, 2006). Binding of densin to the NT domain may mimic the effect of these deletions because densin not only increases the number of functional channels, but also their relative open probability (Fig.

3). Deletion of a CaMKII-binding site in the $Ca_v1.2$ NT domain decreases cell surface $Ca_v1.2$ protein, but increases $Ca_v1.2$ current density in tsA-201 cells (Simms et al., 2015). Although the effect of densin in our transfected cell recordings did not require CaMKII (Fig. 2*B*), we cannot discount the possibility that densin modulates the interaction of CaMKII with neuronal $Ca_v1.2$ channels. CaMKII binds to the α_1 and β subunit of $Ca_v1.2$, which facilitates channel opening (Hudmon et al., 2005; Koval et al., 2010). Densin may alter such interactions because it enhances CaMKII binding to α-actinin (Walikonis et al., 2001; Robison et al., 2005), but can modulate CaMKII phosphorylation of AMPA and NMDA receptors differentially (Jiao et al., 2011).

Although $Ca_v1.2$ undergoes activity-dependent endocytosis in neurons (Green et al., 2007; Hall et al., 2013), the basal turnover rate of $Ca_v1.2$ channels in dendritic spines is slow (>1 h) and their lateral mobility is restricted (Di Biase et al., 2011). The stability of postsynaptic $Ca_v1.2$ channels could be due to their interactions with a variety of proteins in dendritic spines. For example, α-actinin and AKAP79/150 maintain the localization (Hall et al., 2013) and activity (Oliveria et al., 2007) of $Ca_v1.2$ in spines, respectively. However, activation of NMDA receptors causes a redistribution of α-actinin and AKAP79/150 into the dendritic shaft without affecting the localization of $Ca_v1.2$ in the spine (Di Biase et al., 2008), suggesting that these proteins are not sufficient for stabilizing dendritic $Ca_v1.2$ channels. In addition to CaMKII and α-actinin (Strack et al., 2000; Walikonis et al., 2001), densin interacts with Shank (Quitsch et al., 2005), δ-catenin (Izawa et al., 2002), and spinophilin (Baucum et al., 2010). Densin may help to anchor $Ca_v1.2$ channels within a network of interacting proteins, the dissolution of which may cause the loss of cell surface $Ca_v1.2$ channels in brain slices and neurons from densin KO mice (Fig. 7). This mechanism may explain how densin also promotes the dendritic clustering $Ca_v1.3$ (Stanika et al., 2016) despite binding to a different site than $Ca_v1.2$ (Fig. 1*C*,*E*).

The intracellular accumulation of $Ca_v1.2$-HA-ΔNT in the dendritic shaft, as well as its exclusion from spines (Fig. 6*D*), is similar to that of $Ca_v1.2$ mutants deficient in interactions with the auxiliary β subunit (Obermair et al., 2010). Considering that the forward trafficking of SNAP-tagged $Ca_v1.2$ channels in HEK293T cells is accelerated by densin (Fig. 5), densin may play a similar role as the β subunit in facilitating the export of $Ca_v1.2$ channels from their sites of synthesis and insertion into the postsynaptic membrane. This effect of densin may be particularly important to replenish $Ca_v1.2$ channels endocytosed during high levels of neuronal excitation (Green et al., 2007; Hall et al., 2013). The NT of $Ca_v1.2$ contains binding sites for multiple proteins including calmodulin (Ivanina et al., 2000), CaMKII (Simms et al., 2015), and CaBP1 (Zhou et al., 2005). Therefore, the loss of $Ca_v1.2$-HA-ΔNT interactions with densin and potentially other proteins could have collectively contributed to the complete absence of cell surface labeling of these mutant channels in dendrites (Fig. 6*D*).

As one of the major CaMKII-binding proteins in postsynaptic density (Apperson et al., 1996; Strack et al., 2000; Walikonis et al., 2001; Carlisle et al., 2011; Lowenthal et al., 2015), densin may provide a local pool of CaMKII that is necessary for coupling Ca_v1 channels to the activation of CREB in the nucleus (Wheeler et al., 2008; Wheeler et al., 2012). Ca^{2+} influx through Ca_v1 channels is sensed by calmodulin, which binds to and causes autophosphorylation of CaMKII, followed by a series of events leading to translocation of calmodulin to the nucleus and phosphorylation of CREB (Ma et al., 2014). Consistent with a role for densin in positioning CaMKII close to Ca_v1-mediated Ca^{2+} signals, the level of autophosphorylated CaMKII is profoundly reduced (~75%) in neurons from densin KO compared with WT mice (Carlisle et al., 2011). Therefore, densin may not only ensure a sufficient density of $Ca_v1.2$ channels, but also of associated CaMKII enzymes available for excitation–transcription coupling. This would explain the strong reductions in Ca_v1-mediated pCREB induction in densin KO neurons (Fig. 8) and upon shRNA knockdown of densin in hippocampal neurons (Wheeler et al., 2012).

Our results suggest a potential mechanism to account for the overlap in the behavioral phenotypes of densin KO mice and those in mice with targeted deletion of $Ca_v1.2$. Compared with the respective control mice, anxiety-like behavior is significantly greater in densin KO mice (Carlisle et al., 2011) and mice lacking $Ca_v1.2$ expression in the prefrontal cortex (Lee et al., 2012). Anxiety disorders are common in patients with schizophrenia (Achim et al., 2011) and other neuropsychiatric disorders linked to polymorphisms in the *CACNA1C* gene encoding $Ca_v1.2$ (Heyes et al., 2015). It is tempting to speculate that the reduced abundance of functional $Ca_v1.2$ channels may contribute to the increased anxiety-like behavior and other endophenotypes of schizophrenia in densin KO mice (Carlisle et al., 2011). Indeed, molecular analyses of schizophrenia-associated polymorphisms in an intronic region of *CACNA1C* suggest the potential for altered levels of *CACNA1C* expression in patients harboring these variants (Eckart et al., 2016). Therefore, densin KO mice may serve as an appropriate mouse model with which to study how loss of function of $Ca_v1.2$ leads to cellular and behavioral anomalies underlying mental illness.

References

Achim AM, Maziade M, Raymond E, Olivier D, Mérette C, Roy MA (2011) How prevalent are anxiety disorders in schizophrenia? A meta-analysis and critical review on a significant association. Schizophr Bull 37:811–821. CrossRef Medline

Altier C, Dubel SJ, Barrère C, Jarvis SE, Stotz SC, Spaetgens RL, Scott JD, Cornet V, De Waard M, Zamponi GW, Nargeot J, Bourinet E (2002) Trafficking of L-type calcium channels mediated by the postsynaptic scaffolding protein AKAP79. J Biol Chem 277:33598–33603. CrossRef Medline

Apperson ML, Moon IS, Kennedy MB (1996) Characterization of densin-180, a new brain-specific synaptic protein of the O-sialoglycoprotein family. J Neurosci 16:6839–6852. Medline

Baucum AJ 2nd, Jalan-Sakrikar N, Jiao Y, Gustin RM, Carmody LC, Tabb DL, Ham AJ, Colbran RJ (2010) Identification and validation of novel spinophilin-associated proteins in rodent striatum using an enhanced ex vivo shotgun proteomics approach. Mol Cell Proteomics 9:1243–1259. CrossRef Medline

Calin-Jageman I, Lee A (2008) Ca_v1 L-type Ca^{2+} channel signaling complexes in neurons. J Neurochem 105:573–583. CrossRef Medline

Calin-Jageman I, Yu K, Hall RA, Mei L, Lee A (2007) Erbin enhances voltage-dependent facilitation of $Ca_v1.3$ Ca^{2+} channels through relief of an autoinhibitory domain in the $Ca_v1.3$ α_1 subunit. J Neurosci 27:1374–1385. CrossRef Medline

Carlisle HJ, Luong TN, Medina-Marino A, Schenker L, Khorosheva E, Indersmitten T, Gunapala KM, Steele AD, O'Dell TJ, Patterson PH, Kennedy MB (2011) Deletion of densin-180 results in abnormal behaviors associated with mental illness and reduces mGluR5 and DISC1 in the postsynaptic density fraction. J Neurosci 31:16194–16207. CrossRef Medline

Clark NC, Nagano N, Kuenzi FM, Jarolimek W, Huber I, Walter D, Wietzorrek G, Boyce S, Kullmann DM, Striessnig J, Seabrook GR (2003) Neurological phenotype and synaptic function in mice lacking the $Ca_V1.3$ alpha subunit of neuronal L-type voltage-dependent Ca^{2+} channels. Neuroscience 120:435–442. CrossRef Medline

Cox B, Emili A (2006) Tissue subcellular fractionation and protein extraction for use in mass-spectrometry-based proteomics. Nat Protoc 1:1872–1878. CrossRef Medline

Cross-Disorder Group of the Psychiatric Genomics Consortium (2013) Identification of risk loci with shared effects on five major psychiatric

disorders: a genome-wide analysis. Lancet 381:1371–1379. CrossRef Medline

Deisseroth K, Mermelstein PG, Xia H, Tsien RW (2003) Signaling from synapse to nucleus: the logic behind the mechanisms. Curr Opin Neurobiol 13:354–365. CrossRef Medline

Di Biase V, Obermair GJ, Szabo Z, Altier C, Sanguesa J, Bourinet E, Flucher BE (2008) Stable membrane expression of postsynaptic CaV1.2 calcium channel clusters is independent of interactions with AKAP79/150 and PDZ proteins. J Neurosci 28:13845–13855. CrossRef Medline

Di Biase V, Tuluc P, Campiglio M, Obermair GJ, Heine M, Flucher BE (2011) Surface traffic of dendritic CaV1.2 calcium channels in hippocampal neurons. J Neurosci 31:13682–13694. CrossRef Medline

Eckart N, Song Q, Yang R, Wang R, Zhu H, McCallion AS, Avramopoulos D (2016) Functional characterization of schizophrenia-associated variation in CACNA1C. PLoS One 11:e0157086. CrossRef Medline

Flucher BE, Andrews SB, Fleischer S, Marks AR, Caswell A, Powell JA (1993) Triad formation: organization and function of the sarcoplasmic reticulum calcium release channel and triadin in normal and dysgenic muscle in vitro. J Cell Biol 123:1161–1174. CrossRef Medline

Green EM, Barrett CF, Bultynck G, Shamah SM, Dolmetsch RE (2007) The tumor suppressor eIF3e mediates calcium-dependent internalization of the L-Type calcium channel $Ca_v1.2$. Neuron 55:615–632. CrossRef Medline

Gregory FD, Bryan KE, Pangršič T, Calin-Jageman IE, Moser T, Lee A (2011) Harmonin inhibits presynaptic $Ca_v1.3$ Ca^{2+} channels in mouse inner hair cells. Nat Neurosci 14:1109–1111. CrossRef Medline

Gregory FD, Pangrsic T, Calin-Jageman IE, Moser T, Lee A (2013) Harmonin enhances voltage-dependent facilitation of Cav1.3 channels and synchronous exocytosis in mouse inner hair cells. J Physiol 591:3253–3269. CrossRef Medline

Hall DD, Dai S, Tseng PY, Malik Z, Nguyen M, Matt L, Schnizler K, Shephard A, Mohapatra DP, Tsuruta F, Dolmetsch RE, Christel CJ, Lee A, Burette A, Weinberg RJ, Hell JW (2013) Competition between alpha-actinin and Ca^{2+}-calmodulin controls surface retention of the L-type Ca^{2+} channel $Ca_v1.2$. Neuron 78:483–497. CrossRef Medline

Heyes S, Pratt WS, Rees E, Dahimene S, Ferron L, Owen MJ, Dolphin AC (2015) Genetic disruption of voltage-gated calcium channels in psychiatric and neurological disorders. Prog Neurobiol 134:36–54. CrossRef Medline

Hudmon A, Schulman H, Kim J, Maltez JM, Tsien RW, Pitt GS (2005) CaMKII tethers to L-type Ca^{2+} channels, establishing a local and dedicated integrator of Ca^{2+} signals for facilitation. J Cell Biol 171:537–547. CrossRef Medline

Ivanina T, Blumenstein Y, Shistik E, Barzilai R, Dascal N (2000) Modulation of L-type Ca^{2+} channels by $G\beta\gamma$ and calmodulin via interactions with N and C termini of alpha 1C. J Biol Chem 275:39846–39854. CrossRef Medline

Izawa I, Nishizawa M, Ohtakara K, Inagaki M (2002) Densin-180 interacts with delta-catenin/neural plakophilin-related armadillo repeat protein at synapses. J Biol Chem 277:5345–5350. CrossRef Medline

Jenkins MA, Christel CJ, Jiao Y, Abiria S, Kim KY, Usachev YM, Obermair GJ, Colbran RJ, Lee A (2010) Ca^{2+}-dependent facilitation of $Ca_v1.3$ Ca^{2+} channels by densin and Ca^{2+}/calmodulin-dependent protein kinase II. J Neurosci 30:5125–5135. CrossRef Medline

Jiao Y, Robison AJ, Bass MA, Colbran RJ (2008) Developmentally regulated alternative splicing of densin modulates protein-protein interaction and subcellular localization. J Neurochem 105:1746–1760. CrossRef Medline

Jiao Y, Jalan-Sakrikar N, Robison AJ, Baucum AJ 2nd, Bass MA, Colbran RJ (2011) Characterization of a central Ca2+/calmodulin-dependent protein kinase IIalpha/beta binding domain in densin that selectively modulates glutamate receptor subunit phosphorylation. J Biol Chem 286:24806–24818. CrossRef Medline

Kanevsky N, Dascal N (2006) Regulation of maximal open probability is a separable function of Ca(v)beta subunit in L-type Ca2+ channel, dependent on NH2 terminus of alpha1C (Ca(v)1.2alpha). J Gen Physiol 128:15–36. CrossRef Medline

Keppler A, Pick H, Arrivoli C, Vogel H, Johnsson K (2004) Labeling of fusion proteins with synthetic fluorophores in live cells. Proc Natl Acad Sci U S A 101:9955–9959. CrossRef Medline

Koschak A, Reimer D, Huber I, Grabner M, Glossmann H, Engel J, Striessnig J (2001) α_{1D} ($Ca_v1.3$) subunits can form L-type Ca^{2+} channels activating at negative voltages. J Biol Chem 276:22100–22106. CrossRef Medline

Koval OM, Guan X, Wu Y, Joiner ML, Gao Z, Chen B, Grumbach IM, Luczak ED, Colbran RJ, Song LS, Hund TJ, Mohler PJ, Anderson ME (2010) CaV1.2 beta-subunit coordinates CaMKII-triggered cardiomyocyte death and afterdepolarizations. Proc Natl Acad Sci U S A 107:4996–5000. CrossRef Medline

Kurschner C, Yuzaki M (1999) Neuronal interleukin-16 (NIL-16): a dual function PDZ domain protein. J Neurosci 19:7770–7780. Medline

Kurschner C, Mermelstein PG, Holden WT, Surmeier DJ (1998) CIPP, a novel multivalent PDZ domain protein, selectively interacts with Kir4.0 family members, NMDA receptor subunits, neurexins, and neuroligins. Mol Cell Neurosci 11:161–172. CrossRef Medline

Lacinova L, Moosmang S, Langwieser N, Hofmann F, Kleppisch T (2008) Cav1.2 calcium channels modulate the spiking pattern of hippocampal pyramidal cells. Life Sci 82:41–49. CrossRef Medline

Lee AS, Ra S, Rajadhyaksha AM, Britt JK, De Jesus-Cortes H, Gonzales KL, Lee A, Moosmang S, Hofmann F, Pieper AA, Rajadhyaksha AM (2012) Forebrain elimination of cacna1c mediates anxiety-like behavior in mice. Mol Psychiatry 17:1054–1055. CrossRef Medline

Lipscombe D, Allen SE, Toro CP (2013) Control of neuronal voltage-gated calcium ion channels from RNA to protein. Trends Neurosci 36:598–609. CrossRef Medline

Lorenzon NM, Foehring RC (1995) Characterization of pharmacologically identified voltage-gated calcium channel currents in acutely isolated rat neocortical neurons. II. Postnatal development. J Neurophysiol 73:1443–1451. Medline

Lowenthal MS, Markey SP, Dosemeci A (2015) Quantitative mass spectrometry measurements reveal stoichiometry of principal postsynaptic density proteins. J Proteome Res 14:2528–2538. CrossRef Medline

Ma H, Groth RD, Cohen SM, Emery JF, Li B, Hoedt E, Zhang G, Neubert TA, Tsien RW (2014) gammaCaMKII shuttles Ca^{2+}/CaM to the nucleus to trigger CREB phosphorylation and gene expression. Cell 159:281–294. CrossRef Medline

Moosmang S, Haider N, Klugbauer N, Adelsberger H, Langwieser N, Müller J, Stiess M, Marais E, Schulla V, Lacinova L, Goebbels S, Nave KA, Storm DR, Hofmann F, Kleppisch T (2005) Role of hippocampal $Ca_v1.2$ Ca^{2+} channels in NMDA receptor-independent synaptic plasticity and spatial memory. J Neurosci 25:9883–9892. CrossRef Medline

Obermair GJ, Szabo Z, Bourinet E, Flucher BE (2004) Differential targeting of the L-type Ca^{2+} channel alpha 1C ($Ca_v1.2$) to synaptic and extrasynaptic compartments in hippocampal neurons. Eur J Neurosci 19:2109–2122. CrossRef Medline

Obermair GJ, Schlick B, Di Biase V, Subramanyam P, Gebhart M, Baumgartner S, Flucher BE (2010) Reciprocal interactions regulate targeting of calcium channel beta subunits and membrane expression of alpha1 subunits in cultured hippocampal neurons. J Biol Chem 285:5776–5791. CrossRef Medline

Oliveria SF, Dell'Acqua ML, Sather WA (2007) AKAP79/150 anchoring of calcineurin controls neuronal L-type Ca^{2+} channel activity and nuclear signaling. Neuron 55:261–275. CrossRef Medline

Olson PA, Tkatch T, Hernandez-Lopez S, Ulrich S, Ilijic E, Mugnaini E, Zhang H, Bezprozvanny I, Surmeier DJ (2005) G-protein-coupled receptor modulation of striatal $Ca_V1.3$ L-type Ca^{2+} channels is dependent on a Shank-binding domain. J Neurosci 25:1050–1062. CrossRef Medline

Pinggera A, Striessnig J (2016) Cav 1.3 (CACNA1D) L-type Ca^{2+} channel dysfunction in CNS disorders. J Physiol 594:5839–5849. CrossRef Medline

Quitsch A, Berhörster K, Liew CW, Richter D, Kreienkamp HJ (2005) Postsynaptic shank antagonizes dendrite branching induced by the leucine-rich repeat protein Densin-180. J Neurosci 25:479–487. CrossRef Medline

Robertson SD, Matthies HJ, Owens WA, Sathananthan V, Christianson NS, Kennedy JP, Lindsley CW, Daws LC, Galli A (2010) Insulin reveals Akt signaling as a novel regulator of norepinephrine transporter trafficking and norepinephrine homeostasis. J Neurosci 30:11305–11316. CrossRef Medline

Robison AJ, Bass MA, Jiao Y, MacMillan LB, Carmody LC, Bartlett RK, Colbran RJ (2005) Multivalent interactions of calcium/calmodulin-dependent protein kinase II with the postsynaptic density proteins NR2B, densin-180, and alpha-actinin-2. J Biol Chem 280:35329–35336. CrossRef Medline

Simms BA, Zamponi GW (2014) Neuronal voltage-gated calcium channels: structure, function, and dysfunction. Neuron 82:24–45. CrossRef Medline

Simms BA, Souza IA, Rehak R, Zamponi GW (2015) The Cav1.2 N termi-

nus contains a CaM kinase site that modulates channel trafficking and function. Pflugers Arch 467:677–686. CrossRef Medline

Sinnegger-Brauns MJ, Hetzenauer A, Huber IG, Renström E, Wietzorrek G, Berjukov S, Cavalli M, Walter D, Koschak A, Waldschütz R, Hering S, Bova S, Rorsman P, Pongs O, Singewald N, Striessnig J (2004) Isoform-specific regulation of mood behavior and pancreatic beta cell and cardiovascular function by L-type Ca^{2+} channels. J Clin Invest 113:1430–1439. CrossRef Medline

Stanika R, Campiglio M, Pinggera A, Lee A, Striessnig J, Flucher BE, Obermair GJ (2016) Splice variants of the CaV1.3 L-type calcium channel regulate dendritic spine morphology. Sci Rep 6:34528. CrossRef Medline

Strack S, Robison AJ, Bass MA, Colbran RJ (2000) Association of calcium/calmodulin-dependent kinase II with developmentally regulated splice variants of the postsynaptic density protein densin-180. J Biol Chem 275:25061–25064. CrossRef Medline

Takahashi SX, Miriyala J, Colecraft HM (2004) Membrane-associated guanylate kinase-like properties of beta-subunits required for modulation of voltage-dependent Ca^{2+} channels. Proc Natl Acad Sci U S A 101:7193–7198. CrossRef Medline

Tippens AL, Pare JF, Langwieser N, Moosmang S, Milner TA, Smith Y, Lee A (2008) Ultrastructural evidence for pre- and post-synaptic localization of $Ca_v1.2$ L-type Ca^{2+} channels in the rat hippocampus. J Comp Neurol 506:569–583. CrossRef Medline

Walikonis RS, Oguni A, Khorosheva EM, Jeng CJ, Asuncion FJ, Kennedy MB (2001) Densin-180 forms a ternary complex with the a-subunit of Ca^{2+}/calmodulin-dependent protein kinase II and a-actinin. J Neurosci 21:423–433. Medline

Wei X, Neely A, Lacerda AE, Olcese R, Stefani E, Perez-Reyes E, Birnbaumer L (1994) Modification of Ca^{2+} channel activity by deletions at the carboxyl terminus of the cardiac α_1 subunit. J Biol Chem 269:1635–1640. Medline

Wei X, Neely A, Olcese R, Lang W, Stefani E, Birnbaumer L (1996) Increase in Ca2+ channel expression by deletions at the amino terminus of the cardiac alpha 1C subunit. Receptors Channels 4:205–215. Medline

Weick JP, Groth RD, Isaksen AL, Mermelstein PG (2003) Interactions with PDZ proteins are required for L-type calcium channels to activate cAMP response element-binding protein-dependent gene expression. J Neurosci 23:3446–3456. Medline

Wheeler DG, Barrett CF, Groth RD, Safa P, Tsien RW (2008) CaMKII locally encodes L-type channel activity to signal to nuclear CREB in excitation-transcription coupling. J Cell Biol 183:849–863. CrossRef Medline

Wheeler DG, Groth RD, Ma H, Barrett CF, Owen SF, Safa P, Tsien RW (2012) Ca(V)1 and Ca(V)2 channels engage distinct modes of Ca^{2+} signaling to control CREB-dependent gene expression. Cell 149:1112–1124. CrossRef Medline

White JA, McKinney BC, John MC, Powers PA, Kamp TJ, Murphy GG (2008) Conditional forebrain deletion of the L-type calcium channel Ca V 1.2 disrupts remote spatial memories in mice. Learn Mem 15:1–5. CrossRef Medline

Yang L, Katchman A, Weinberg RL, Abrams J, Samad T, Wan E, Pitt GS, Marx SO (2015) The PDZ motif of the alpha1C subunit is not required for surface trafficking and adrenergic modulation of CaV1.2 channel in the heart. J Biol Chem 290:2166–2174. CrossRef Medline

Zhang H, Maximov A, Fu Y, Xu F, Tang TS, Tkatch T, Surmeier DJ, Bezprozvanny I (2005) Association of $Ca_V1.3$ L-type calcium channels with Shank. J Neurosci 25:1037–1049. CrossRef Medline

Zhou H, Kim SA, Kirk EA, Tippens AL, Sun H, Haeseleer F, Lee A (2004) Ca^{2+}-binding protein-1 facilitates and forms a postsynaptic complex with $Ca_v1.2$ (L-type) Ca^{2+} channels. J Neurosci 24:4698–4708. CrossRef Medline

Zhou H, Yu K, McCoy KL, Lee A (2005) Molecular mechanism for divergent regulation of $Ca_v1.2$ Ca^{2+} channels by calmodulin and Ca^{2+}-binding protein-1. J Biol Chem 280:29612–29619. CrossRef Medline